Correspondence

Optimum Configurations for Static and Rotating Phased Arrays

We introduce a method for comparing the system surveillance characteristics of static and rotating phased array radars that also includes subregions of a given total surveillance area. The search function is obtained for different hemispherical regions based on the number of active/nonactive array faces. We derive the surveillance occupancy functions for a typical scenario consisting of 4 search sectors under various constraints and consider the number of radiating elements required for surveillance purposes. We derive an expression for the accurate determination of the surveillance volume and average beam dwell times for different scan angles based on the theory of manifolds and consider the impact of various window functions on the broadside dwell times.

I. INTRODUCTION

A phased array radar [1] has the ability to perform many tasks, one of the most important being surveillance. In order to perform 360° volumetric surveillance a certain number of array faces N_F is required with each array face consisting of a fixed number (N_{elem}) of transmit (T_x) and receive (R_x) modules, respectively. These array faces are typically inclined at an angle α from the vertical for performance reasons and each array face scans a volume of space bound by angles in elevation (θ_1,θ_2) and azimuth (ϕ_1,ϕ_2), respectively. The azimuth angles that bound the area of surveillance are related to the number of array faces needed to carry out 360° scanning via $N_F = 2\pi/(\phi_2 - \phi_1)$. For example if we require that one array face scan a region bound by $\phi_1 = -60°$ and $\phi_2 = +60°$ on either side of broadside then the number of faces required to perform 360° surveillance is $N_F = 2\pi/120 = 3$ or $N_F = \pi/\phi_{\max} = \pi/60 = 3$. As each array face scans such a surveillance region, a certain amount of time is required which is known as the frame time, i.e., the total time to scan the surveillance area allocated to one array face. If the phased array face scans subregions or different sectors of the total surveillance area, eg., close to the horizon, then the amount of time to do this is defined as the

Manuscript received May 9, 2007; revised November 28, 2007; released for publication March 6, 2008.

IEEE Log No. T-AES/44/4/930738.

Refereeing of this contribution was handled by M. Rangaswamy.

The work of A. Alexopoulos was supported by ILMOMF 9/6-2005.

(surveillance) search function time. There are typically two types of phased array radar systems in use: static phased arrays and rotating phased arrays with each type having better performance characteristics than the other depending on operational requirements. However a mathematical method that allows direct comparison between the two is almost nonexistent. In this correspondence we will derive an approach that allows such a comparison where the measure of performance is the scan rate (time taken) to perform surveillance of different regions/subregions under certain constraints. At the same time we also solve some of the problems associated with arrays in general, that is, the noninvariance of array parameters with scan angle. More precisely, the effective aperture of arrays changes as the radiation beam is steered in elevation and azimuth which dramatically alters (broadens) the beamwidth and hence the gain or signal-to-noise ratio (SNR) from that at broadside. Furthermore the beam at broadside is given a dwell time t_B which is the amount of time it spends on a target for example. Due to the loss in SNR for scanning off broadside the beam dwell time is not invariant and must increase in order to match the initial value at broadside. This effect has a direct impact on the search function time. In addition, there is difficulty in determiming the number of beams due the beam-broadening effect and each beam direction has to be calculated explicitly. Not least of all, the array tilt angle α makes it even more difficult to determine the surveillance area since it "distorts" the bounding regions of the scanned area. Various attempts have been made to address some of these issues mainly for static arrays [2–5] that involve unnecessarily complicated iterative techniques, but a more general and simplified approach is lacking. In this correspondence we derive results that solve the issues addressed above, thus allowing the two radar types to be compared without the need for complex iterative or nontractable approaches. Specifically, we examine the number of radiating elements that are required in order that surveillance of different hemispherical regions and subregions is achieved. In particular we define occupancy functions for different subregions but before doing so, it is necessary to derive the search functions for these regions/subregions which in the end allow us to compare static and rotating array broadside dwell times that are required for surveillance under certain constraints. We derive an expression for the accurate determination of the area scanned by static and rotating phased arrays as well as the average beam dwell times for arbitrary scan angles in uv-space [5]. We use transformations that involve the tilt angle of the arrays and in the case of rotating arrays we make use of a pseudocylindrical coordinate system [6]. We make use of weighting functions and consider how these effect the broadside dwell times used to do surveillance in different regions/subregions.

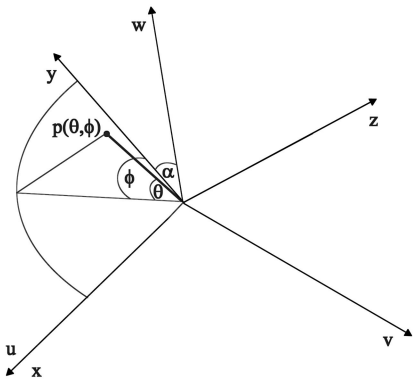

Fig. 1. Coordinate system for static arrays relating the real coordinate system (x,y,z) (polar) to (u,v,w) reference system centered on array face. Scanning vector $p(\theta,\phi)$ determines the beam position, i.e., $p(\theta,\phi;\alpha)\rightarrow\gamma$; see (22). Array tilt angle α is shown as rotation between array face with coordinates (u,v,w) and real world coordinate system (x,y,z).

II. THE SEARCH FUNCTION

For an array tilt angle α we can obtain coordinate transformations that relate the real world elevation θ and azimuth ϕ to the uv-space coordinate system. For a static array whose axes form a basis on the array face, i.e., the uv-plane (see Fig. 1), we have [7]

$$u=\cos(\theta)\sin(\phi) \tag{1}$$

and

$$v=\sin(\theta)\cos(\alpha)-\cos(\theta)\cos(\phi)\sin(\alpha). \tag{2}$$

In a similar way we define coordinate transformations for a rotating array that are based on pseudocylindrical coordinates commonly known as Sanson-Flamsteed projections [6]. Relating the pseudocylindrical u^*v^*-space to the real world elevation and azimuth we have

$$u^*=\phi\cos(\theta) \tag{3}$$

and

$$v^*=\sin(\theta)\cos(\alpha)-\cos(\theta)\sin(\alpha)\equiv\sin(\theta-\alpha). \tag{4}$$

Note that "*" denotes rotating arrays and not the complex conjugate. The invariance of the beamwidth for all scan angles under these transformations means that we can define the area to be a function of the broadside half-power beamwidth or any other overlap angle of choice ψ:

$$A_{\text{beams}}=\pi\sin^2\left(\frac{\psi}{2}\right). \tag{5}$$

It has been shown [8] that the number of beams required to scan a volume of space for one static array face as a function of the total number of array faces N_F required to do hemispherical surveillance is

$$N_{\text{beams}}=\frac{\Omega}{2\pi N_F}\csc^2\left(\frac{\psi}{2}\right) \tag{6}$$

where

$$\Omega = \pi \sin(\alpha)(\cos(2\theta_1) - \cos(2\theta_2)) + N_F \cos(\alpha) \times \sin(\pi/N_F)(\sin(2\theta_2) - \sin(2\theta_1) + 2(\theta_2 - \theta_1)) \tag{7}$$

and in the case of one rotating array face

$$N^*_{\text{beams}} = \frac{\Omega^*}{2N_F} \csc^2\left(\frac{\psi}{2}\right) \tag{8}$$

where

$$\Omega^* = \sin(\alpha - 2\theta_1) - \sin(\alpha - 2\theta_2) + 2\cos(\alpha)(\theta_2 - \theta_1). \tag{9}$$

Here the number of array faces is related to the maximum azimuth extent $\phi_{\max}$ for one array face by $N_F = \pi/\phi_{\max}$, α is the array tilt angle, and $\theta_{1,2}$ are the elevations bounding surveillance. We are now faced with the challenge of obtaining an accurate measure of the surveillance area (volume). It is evident that the surveillance area is represented by a manifold or surface above the real coordinate system (x, y, z). As an analogy consider the longitude and latitude geodesics of the Earth which are curves that are especially pronounced towards the zenith with added complication when we include the array tilt angle α. Thus an accurate determination of the surveillance region requires finding the area of such a bound manifold. Since we require that the beamwidths remain invariant during scanning we have made the transformation to the coordinate system of the array face, i.e., (u, v, w). It is in this latter coordinate system that the beamwidths remain invariant, at least from a geometric point of view, and which will allow us to obtain an accurate average beam dwell time by weighting the manifold by the surveillance area. In $uv(u^*v^*)$-space let the surveillance area (manifold) be represented by a function $\mathbf{f} = \mathbf{f}(u(r,\theta,\phi), v(r,\theta,\phi)) \equiv \mathbf{f}(u(\theta,\phi), v(\theta,\phi))$ since in this coordinate system we can take the value $r = 1$. In order to obtain the surveillance area A_{uv} (or $A_{u^*v^*}$) we notice that any two vectors $\mathbf{t}_1$ and $\mathbf{t}_2$ on the surface of the manifold are not orthogonal to each other but rather span as vectors in a parallelogram with tangent components $\mathbf{t}_1 = \partial\mathbf{r}/\partial\theta\, d\theta$ and $\mathbf{t}_2 = \partial\mathbf{r}/\partial\phi\, d\phi$ where $\mathbf{r} = (u, v, 0)$. The area of the small parallelogram is the magnitude of the crossproduct $\|\mathbf{t}_1 \times \mathbf{t}_2\|$, which simplifies to (note: the analysis that follows also applies to rotating arrays u^*v^* unless we specify otherwise):

$$dA_{uv} = \|(\partial\mathbf{r}/\partial\theta) \times (\partial\mathbf{r}/\partial\phi)\| d\theta\, d\phi \tag{10}$$

where dA_{uv} is the surface area differential for the surface. Equation (10) is justified thus: If dA_{uv} maps a region S in the uv-plane to the surface of the surveillance manifold Σ (or vice-versa), then it follows that a partition of S in the uv-plane leads to a partition of Σ in which each partition is practically the same as the parallelogram spanned by $(\partial\mathbf{r}/\partial\theta)\Delta\theta_j$ and $(\partial\mathbf{r}/\partial\phi)\Delta\phi_k$. The area of the parallelogram that is spanned is $\Delta A_{jk} = \|(\partial\mathbf{r}/\partial\theta) \times (\partial\mathbf{r}/\partial\phi)\| \Delta\theta_j \Delta\phi_k$, so that the approximate area of the surface becomes

$$A_{uv} \approx \sum_{j=1}^{n}\sum_{k=1}^{m} \Delta A^{(jk)}_{uv} = \sum_{j=1}^{n}\sum_{k=1}^{m} \left\| \left(\frac{\partial\mathbf{r}}{\partial\theta}\right) \times \left(\frac{\partial\mathbf{r}}{\partial\phi}\right) \right\| \Delta\theta_j \Delta\phi_k. \tag{11}$$

In the limit where the partition becomes finer and finer the limit of the Riemann sum from (11) then becomes

$$A_{uv} = \int_S \int dA_{uv} = \int_S \int \left\| \left(\frac{\partial\mathbf{r}}{\partial\theta}\right) \times \left(\frac{\partial\mathbf{r}}{\partial\phi}\right) \right\| d\theta\, d\phi. \tag{12}$$

Equation (12) determines the area scanned by the array but we will transform it explicitly to a form that only requires solution of the Jacobian coordinate transformation matrix using the conformal transformations given by (1), (2), (3), and (4). Let the ith component of the cross-product of two vectors be $(\mathbf{v}_1 \times \mathbf{v}_2)^i = \epsilon_{ijk} v_1^j v_2^k$, where repeated indices are summed, then we have

$$\begin{aligned}
|\mathbf{v}_1 \times \mathbf{v}_2|^2 &= (\mathbf{v}_1 \times \mathbf{v}_2)^i (\mathbf{v}_1 \times \mathbf{v}_2)^i \\
&= (\varepsilon_{ijk} v_1^j v_2^k)(\varepsilon_{ilm} v_1^l v_2^m) \\
&= \varepsilon_{ijk}\varepsilon_{ilm} v_1^j v_2^k v_1^l v_2^m \\
&= (\delta_{jl}\delta_{km} - \delta_{jm}\delta_{kl}) v_1^j v_2^k v_1^l v_2^m \\
&= \delta_{jl}\delta_{km} v_1^j v_2^k v_1^l v_2^m - \delta_{jm}\delta_{kl} v_1^j v_2^k v_1^l v_2^m \\
&= v_1^j v_2^k v_1^j v_2^k - v_1^j v_2^k v_1^k v_2^j \\
&= (v_1^j v_1^j)(v_2^k v_2^k) - (v_1^j v_2^j)(v_1^k v_2^k) \\
&= |\mathbf{v}_1|^2 |\mathbf{v}_2|^2 - (\mathbf{v}_1 \cdot \mathbf{v}_2)^2
\end{aligned} \tag{13}$$

where δ_{xy} is the Kroneker delta-function and ϵ_{xyz} is the Levi-Civita or alternating tensor with

$$\epsilon_{\alpha\beta\gamma} = \begin{cases} +1 & \alpha\beta\gamma \text{ is an even permutation of } (1,2,3) \\ -1 & \alpha\beta\gamma \text{ is an odd permutation of } (1,2,3) \\ 0 & \text{otherwise} \end{cases}. \tag{14}$$

If we consider a $(1,1)$-tensor A^i_j we can obtain a tensor C^i_j if

$$C^i_j \equiv [A^T]^i_k A^k_j = A^k_i A^k_j \tag{15}$$

where A^T is the transpose of A. Let A be a matrix such that its elements are composed of the vectors $\mathbf{v}_1$ and $\mathbf{v}_2$:

$$\mathbf{A} = \begin{pmatrix} \mathbf{v}_1 & \mathbf{v}_2 \\ \mathbf{0} & \mathbf{0} \end{pmatrix} \tag{16}$$

then from (15) we have that the determinant is

$$\begin{aligned}\det|\mathbf{A}^T\mathbf{A}| &= C_1^1C_2^2 - C_2^1C_1^2 \\ &= (\mathbf{v}_1\cdot\mathbf{v}_1)(\mathbf{v}_2\cdot\mathbf{v}_2) - (\mathbf{v}_1\cdot\mathbf{v}_2)^2 \\ &= |\mathbf{v}_1|^2|\mathbf{v}_2|^2 - (\mathbf{v}_1\cdot\mathbf{v}_2)^2. \end{aligned} \tag{17}$$

Equating (13) and (17) we see that

$$\det|\mathbf{A}^T\mathbf{A}| = |\mathbf{v}_1\times\mathbf{v}_2|^2. \tag{18}$$

Since the cross-product of two vectors can be formulated based on the Jacobian matrix we define the matrix $\mathbf{A}$ in (18) as the Jacobian.[1] Thus the surveillance region scanned in real space is mapped on to the $uv(u^*v^*)$-space coordinate system which we then project on to the $uv(u^*v^*)$-plane and with the use of the coordinate transformations we define the area for both static and rotating phased arrays to be (for the appropriate choice of coordinates uv or u^*v^*):

$$A_{uv} = \int_{\phi_1}^{\phi_2}\int_{\theta_1}^{\theta_2}\sqrt{\det\left|\left[\frac{\partial(u,v)}{\partial(\theta,\phi)}\right]^T\left[\frac{\partial(u,v)}{\partial(\theta,\phi)}\right]\right|}\,d\theta\,d\phi \tag{19}$$

where T is the transpose operator, $\phi_1 = -\pi/N_F$ and $\phi_2 = \pi/N_F$ are the azimuth angles, and $\partial(u,v)/\partial(\theta,\phi)$ (or $\partial(u^*,v^*)/\partial(\theta,\phi)$) represents the Jacobian matrix,

$$\frac{\partial(u,v)}{\partial(\theta,\phi)} = \begin{pmatrix}\partial u/\partial\theta & \partial u/\partial\phi \\ \partial v/\partial\theta & \partial v/\partial\phi\end{pmatrix}. \tag{20}$$

From the angular bounds we can obtain the frame time which is the total time required to scan the total surveillance region. Furthermore any subregion has an associated time that is required to cover it, i.e., the search function time for that subregion. We can obtain both of these by considering the average beam dwell time $\langle\tau'\rangle = t_B\langle\tau\rangle$ for each of the beam directions where t_B is the beam dwell time at broadside and in the case of static arrays we have

$$\langle\tau\rangle = \frac{1}{A_{uv}}\int_{\phi_1}^{\phi_2}\int_{\theta_1}^{\theta_2}\frac{1}{\cos^3(\gamma)}\det\left|\frac{\partial(u,v)}{\partial(\theta,\phi)}\right|d\theta\,d\phi \tag{21}$$

where

$$\gamma = \sin^{-1}\left(\sqrt{\sin^2(\theta-\alpha)+\cos^2(\theta-\alpha)\sin^2(\phi)}\right) \tag{22}$$

Similarly for a rotating phased array the average beam dwell time is given by $\langle\tau^{*'}\rangle = t_B\langle\tau^*\rangle$ where

$$\langle\tau^*\rangle = \frac{1}{\delta}\int_{\theta_1}^{\theta_2}\frac{1}{\cos^3(\theta-\alpha)}\frac{\partial v^*}{\partial\theta}d\theta \tag{23}$$

where $\delta = \sin(\theta_2-\alpha) - \sin(\theta_1-\alpha)$ and we note that there is only dependence on the elevation and not on the azimuth, i.e., ϕ is a constant. Equations (21) and (23) contain the factor $1/\cos^3(.)$ where the power 3 is chosen in order to account for two-way loss effects [9]. Note that $\langle\tau\rangle$ and $\langle\tau^*\rangle$ in (21) and (23), respectively, do not represent true time quantities but can be thought of as being dimensionless(normalised) averages of time-like manifolds that describe geometrical changes in the beam dwell times and which, after being multiplied by t_B, give the average beam dwell times $\langle\tau'\rangle$ and $\langle\tau^{*'}\rangle$ as required. From the average dwell time and the number of beams we can derive the search function time to perform the surveillance task in any subregion as $\tau_s = t_B\langle\tau\rangle N_{\text{beams}}$ or $\tau_s^* = t_B\langle\tau^*\rangle N_{\text{beams}}^*$. Fig. 2 shows the average beam dwell times, for static and rotating arrays as a function of the array tilt angle α. In Table I and Table II for the parameters given, we compare the number of beams, average dwell times and search function times for different static and rotating array faces. The search function times for static arrays are always greater than those for rotating arrays. Interestingly, the average dwell times for rotating arrays are constant and the values "cluster" around the broadside dwell time $t_B = 1$ ms. This is due to the fact that the scanning is in elevation only with no azimuth scanning (constant) so the only contribution comes from averaging the beam dwell times in elevation.

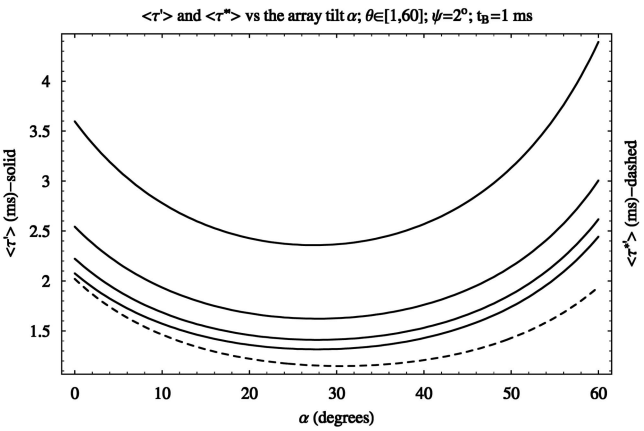

Fig. 2. For overlap beam angle $\psi = 2°$, broadside dwell time $t_B = 1$ ms and elevation angles in range (1–60) deg we show change of average beam dwell time $\langle\tau'\rangle$ and $\langle\tau^{*'}\rangle$ for static and rotating arrays, respectively, as function of the array tilt angle α. Solid curves represent static arrays with azimuth bounds given by number of faces N_F required to do hemispherical surveillance. Top curve is for $N_F = 3$ and minimum beam dwell time $\min(\langle\tau'\rangle) = 2.358$ ms. Below that is the case for $N_F = 4$ with $\min(\langle\tau'\rangle) = 1.623$ ms and then $N_F = 5$ with $\min(\langle\tau'\rangle) = 1.411$ ms. Lowest curve is for $N_F = 6$ with $\min(\langle\tau'\rangle) = 1.316$ ms. Dashed curve has lowest average beam dwell times and represents rotating array case for all N_F since there is no dependence in azimuth direction and only on elevation. Minimum of curve gives value $\min(\langle\tau^{*'}\rangle) = 1.148$ ms.

III. NUMBER OF ELEMENTS REQUIRED FOR SURVEILLANCE

We consider what the number of radiating elements N_{elem} is for a constant broadside dwell time

[1]The proof is straightforward but mathematically tedious.

TABLE I
Static Phased Array with Parameters: t_B = 1 ms; $\alpha = 15°$; $\psi = 1°$; θ = (1–20) deg

No. of Faces: N_F	No. of Beams per Face: N_{beams}	Average Dwell Time per Beam: $\langle\tau'\rangle$ (ms)	Search Function Time per Face: τ_s (s)
3	2301	2.111	4.86
4	1879	1.476	2.77
5	1564	1.285	2.01
6	1331	1.198	1.59

TABLE II
Rotating Phased Array with Parameters: t_B = 1 ms; $\alpha = 15°$; $\psi = 1°$; θ = (1–20) deg

No. of Faces: N_F	No. of Beams per Face: N^*_{beams}	Average Dwell Time per Beam: $\langle\tau^{*\prime}\rangle$ (ms)	Search Function Time per Face: τ^*_s (s)
3	2819	1.023	2.88
4	2115	1.023	2.16
5	1692	1.023	1.73
6	1410	1.023	1.44

t_B in order for static and rotating arrays to perform surveillance. In the analysis that follows we consider the case for static arrays but the same procedure applies to rotating arrays. Since the average beam dwell time as a function of the scan angles (θ,ϕ) is given by $\langle\tau'\rangle = t_B\langle\tau\rangle$ then the frame time τ_{frame} is related to t_B by $t_B = \tau_{\text{frame}}/(\langle\tau\rangle N_{\text{beams}})$. For a single coherent integration we have [10]

$$R^4_{\max} = \frac{\tau_{\text{frame}}}{\langle\tau\rangle N_{\text{beams}}}\frac{P_{\text{av}}\sigma G_t G_r \lambda^2}{(4\pi)^3 kTDL} \tag{24}$$

so that

$$R^4_{\max} = \frac{\tau_{\text{frame}}}{\langle\tau\rangle N_{\text{beams}}}\frac{P_{\text{av}}\sigma A\eta^2}{4\pi^2 kTDL\sin^2(\psi/2)} \tag{25}$$

where P_{av}-average power, λ-wavelength, σ-RCS, L-losses, T-temperature and D-SNR. In (25) we have used (refer also to [10]),

$$G_t = \frac{4\eta}{\sin^2(\psi/2)} \tag{26}$$

and

$$G_r = \frac{4\pi\eta A}{\lambda^2} \tag{27}$$

for the transmit and receive gains where ψ is the arbitrary beam overlap angle such as the 3 dB point and η is the array efficiency. Further transforming (25) by replacing the array power and effective area by the element contributions P_{elem} and A_{elem} gives

$$R^4_{\max} = \frac{\tau_{\text{frame}} N_{\text{use}}}{N_F\langle\tau\rangle N_{\text{beams}}}\frac{N^2_{\text{elem}}P_{\text{elem}}A_{\text{elem}}\sigma\eta^2}{4\pi^2 kTDL\sin^2(\psi/2)}. \tag{28}$$

In (28) we have introduced the factor N_{use}/N_F, where N_F is the number of faces and N_{use} is the number of faces transmitting or receiving simultaneously in the surveillance regions. Since $N_F = \pi/\phi_{\max}$ where $\phi_{\max}$ is the maximum azimuth scanned in any of the regions we finally obtain

$$\frac{N_{\text{elem}}}{\sqrt{\kappa}} = \sin(\psi/2)\left(\frac{\pi\hat{\tau}_s}{\phi_{\max}N_{\text{use}}}\right)^{1/2} \tag{29}$$

where κ is the system-dependent constant

$$\kappa = \frac{4\pi^2 R^4_{\max} kTDL}{\tau_{\text{frame}}P_{\text{elem}}A_{\text{elem}}\sigma\eta^2} \tag{30}$$

and we define $\hat{\tau}_s = \langle\tau\rangle N_{\text{beams}}$, i.e., we have factored out the broadside dwell time t_B from τ_s. It should be noted that the frame time τ_{frame} appearing in (30) is assumed to be constant and is reflected in column 5 of the tabulated results in Table III while in all other cases it is not a constant. Equation (29) describes how the number of elements per face must change in order to maintain a constant free-space surveillance time. Table III gives the total search time to perform 360° surveillance based on the number of array faces in use. The corresponding number of elements for surveillance is also shown. What is interesting to note amongst other things is that the 3-face rotating array system with two active arrays has the same search function time to that of the 6-face system with the three active array faces. In the next section we look at the number of elements required for static and rotating arrays to perform sector scanning. In particular Table VI shows that for $N_F = 3$ in particular, rotating arrays have a smaller number of radiating elements needed for surveillance. As the number of faces increases the difference between the two is very small, especially in subregions r_3 and r_4. This has enormous implications to such things as cost, weight, and cooling of arrays. Interestingly, the number of elements for rotating arrays is constant as N_F increases in the different subregions.

IV. COMPARISON OF SECTOR SURVEILLANCE CHARACTERISTICS

In this section we compare static and rotating radar system performance under sector scanning conditions via the occupancy function. The amount of time required to scan a subregion will dictate how much time is taken from the frame time which subsequently will determine the time that is left over for other applications or tasks, e.g., dedicated tracking. For a frame time τ_{frame} and search function time τ_s we define the occupancy η to be the ratio of the search function time to the frame time required to complete surveillance in a particular subregion, i.e., $\eta = \tau_s/\tau_{\text{frame}}$ or η^* in the case of rotating arrays. We note that if the region required to be scanned is the total surveillance region only, then the occupancy allowed for that task is η = 100 percent. In order to investigate the occupancy profiles between static

TABLE III

Total Search Function Time for t_B = 1 ms (Column 4) and Relative Number of Elements for a Fixed (Noise Limited) Frame Time τ_{frame} (Column 5) for Different Number of Active Array Faces

Parameters: $\alpha = 15°$; $\psi = 1°$; θ = (1–20) deg

Array Type	No. of Faces:	Number of Simultaneously Active Faces:	Total Search Function Time for 360° Surveillance (s):	$N_{\text{elem}}/\sqrt{\kappa}$:
Static	3	1	14.58	1.8250
		2	9.72	1.0537
		3	4.86	0.6083
Static	4	1	11.08	1.8371
		2	8.31	1.1250
		4	2.77	0.4592
Static	6	1	9.54	2.0878
		2	7.95	1.3476
		3	6.36	0.9842
		6	1.59	0.3479
Rotating	3	1	8.64	1.4049
		2	5.76	0.8111
		3	2.88	0.4683
Rotating	4	1	8.64	1.6222
		2	6.48	0.9934
		4	2.16	0.4055
Rotating	6	1	8.64	1.9868
		2	7.20	1.2825
		3	5.76	0.9366
		6	1.44	0.3311

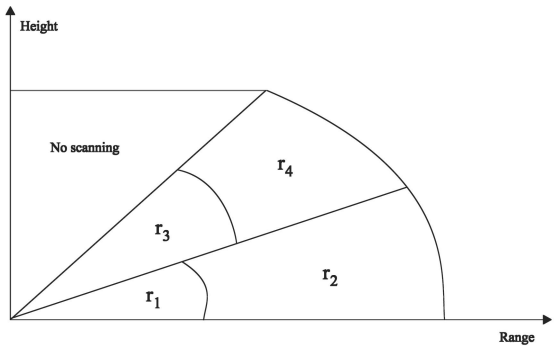

Fig. 3. Typical division of search volume into subregions which can be defined by elevation, azimuth, and range.

and rotating arrays we consider a typical scenario as shown in Fig. 3 for arrays tilted back at an angle $\alpha = 15°$ with a broadside half-power beamwidth of $\psi = 2°$. The subregions r_1, r_2, r_3, and r_4 are examined for the system parameters given in Table IV which represent typical design specifications where the frame times in the different subregions are given and the relative energy required for coherent integration E is dictated by the normalised ratio of the radar cross section σ_0 and the pattern factor F over the range R, i.e., $E \propto (\sigma_0 F^4/R^4)_{\max}$. Using these parameters and the surveillance occupancy functions we can determine what the chosen broadside dwell time t_B should be if all the subregions are scanned with the restrictions imposed in Table IV and with the added constraint that the surveillance be done within a time $t_{\min}$ representing the smallest frame time. In our analysis this is $t_{\min} = 1$ s corresponding to subregion r_1 and it is the value used in this paper. Suppose we factor out t_B from the occupancy function which we redefine to be $\hat{\eta} = N_{\text{beams}}\langle\tau\rangle/\tau_{\text{frame}} \equiv \hat{\tau}_s/\tau_{\text{frame}}$, then the broadside dwell time is obtained from

$$t_B = t_{\min} \Big/ \left[\sum_{j=1}^{N=4} E_j \hat{\eta}_j\right] = \frac{t_{\min}}{E_1\hat{\eta}_1 + E_2\hat{\eta}_2 + E_3\hat{\eta}_3 + E_4\hat{\eta}_4} \tag{31}$$

where j represents the different subregions. Table V shows the search functions for $N_F = 3$, 4, and 5 faced static and rotating phased array radars. Also shown are the broadside dwell times required so that all the subregions are scanned within the constraints given in Table IV and in a time less or equal to $t_{\min}$. As the number of faces increase, so do the broadside dwell times. More precisely, for $N_F = 3$ the subregion search functions are greater due to the larger surveillance angles scanned. This implies that the broadside dwell times must be small in order to compensate and to meet the overall system frame time requirements. For $N_F = 5$ for example, the broadside dwell times are greater because the subregion search functions are smaller due to the smaller angular bounds. In all cases, rotating arrays have greater flexibility in the range of broadside dwell times that can be chosen to cover the same subregions as the static arrays. This is critical if a radar needs a longer broadside dwell time

TABLE IV
An Example of System Parameters and Angular Bounds for the Different Surveillance Subregions of Fig. 3

Subregion: r	Scan Angles in deg for $N_F = 3$	Scan Angles in deg for $N_F = 4$	Scan Angles in deg for $N_F = 5$	Frame Time $\tau_{\text{frame}}(s)$	Relative Energy E
r_1	$0 \le \theta \le \pi/6$ $-\pi/3 \le \phi \le \pi/3$	$0 \le \theta \le \pi/6$ $-\pi/4 \le \phi \le \pi/4$	$0 \le \theta \le \pi/6$ $-\pi/5 \le \phi \le \pi/5$	1	1
r_2	$0 \le \theta \le \pi/6$ $-\pi/3 \le \phi \le \pi/3$	$0 \le \theta \le \pi/6$ $-\pi/4 \le \phi \le \pi/4$	$0 \le \theta \le \pi/6$ $-\pi/5 \le \phi \le \pi/5$	4	2
r_3	$\pi/6 \le \theta \le \pi/3$ $-\pi/6 \le \phi \le \pi/6$	$\pi/6 \le \theta \le \pi/3$ $-\pi/9 \le \phi \le \pi/9$	$\pi/6 \le \theta \le \pi/3$ $-\pi/10 \le \phi \le \pi/10$	2	1
r_4	$\pi/6 \le \theta \le \pi/3$ $-\pi/6 \le \phi \le \pi/6$	$\pi/6 \le \theta \le \pi/3$ $-\pi/9 \le \phi \le \pi/9$	$\pi/6 \le \theta \le \pi/3$ $-\pi/10 \le \phi \le \pi/10$	4	2

TABLE V
Modified Search Function Times $\hat{\tau}_s$ and the Corresponding Broadside Dwell Times Required to Scan the Subregions Under the Constraints of Table IV are Shown for $N_F = 3$, 4, and 5 Face Static and Rotating Phased Arrays

Subregion: r	$\hat{\tau}_s$ for $N_F = 3$	$\hat{\tau}_s$ for $N_F = 4$	$\hat{\tau}_s$ for $N_F = 5$
r_1	static: 1.89827 rotating: 1.12021	static: 1.07971 rotating: 0.84015	static: 0.78111 rotating: 0.67212
r_2	static: 1.89827 rotating: 1.12021	static: 1.07971 rotating: 0.84015	static: 0.78111 rotating: 0.67212
r_3	static: 0.60719 rotating: 0.56755	static: 0.38020 rotating: 0.37837	static: 0.33909 rotating: 0.34053
r_4	static: 0.60719 rotating: 0.56755	static: 0.38020 rotating: 0.37837	static: 0.33909 rotating: 0.34053
t_B	static: 0.28947 rotating: 0.44486	static: 0.50005 rotating: 0.61027	static: 0.66192 rotating: 0.74144

which directly effects how the beam dwell times at arbitrary angles must be changed in order to maintain SNR amongst other things under the restriction that the time is no greater than $t_{\min}$. Note that the values for t_B in Table V have been normalised by $t_{\min}$ and are therefore dimensionless. In Table VI we display the number of elements required in order to perform scanning in the different sectors for varying array faces.

V. EFFECT OF WEIGHTED ARRAYS ON THE BROADSIDE DWELL TIME

In the last two rows of Table V we obtained the broadside dwell time that is required for static and rotating arrays so that the subregions could be scanned in a time interval $t_{\min}$ and under the restrictions of Table IV. This was done using unweighted coefficients appearing in the array factors

$$f(\psi) = 2\sum_{m=1}^{N_{\text{elem}}/2} a_m \cos\left[\left(m - \frac{1}{2}\right)\psi\right] \tag{32}$$

TABLE VI
Number of Radiating Elements Required to Perform Surveillance Based on the Subregion Parameters of Tables IV and V. Here we Take the Case of One Active Array Face

Subregion: r	$N_{\text{elem}}/\sqrt{\kappa}$ for $N_F = 3$	$N_{\text{elem}}/\sqrt{\kappa}$ for $N_F = 4$	$N_{\text{elem}}/\sqrt{\kappa}$ for $N_F = 5$
r_1, r_2	static: 0.31525 rotating: 0.24217	static: 0.27453 rotating: 0.24217	static: 0.26107 rotating: 0.24217
r_3, r_4	static: 0.25214 rotating: 0.24377	static: 0.24436 rotating: 0.24377	static: 0.24326 rotating: 0.24377

for even N_{elem} and

$$f(\psi) = a_0 + 2\sum_{m=1}^{(N_{\text{elem}}-1)/2} a_m \cos[(m\psi)\psi] \tag{33}$$

for odd N_{elem} where $\psi = (2\pi d/\lambda)\cos(\theta) + \alpha$, α is the element phase shift, θ is the radiation angle from the plane of the array, d is the element spacing, and λ is the wavelength. We now consider the case where the window functions appearing in (32) and (33) are not unity and determine an expression that relates the weighted broadside dwell time t_B^w to the unweighted t_B^u for static and rotating arrays (see for example Table V). We use five different window functions namely: Chebyshev, Hamming, Kaiser, Hann, and Blackman-Harris [11–13]. Recalling that $t_B = \tau_{\text{frame}}/(\langle\tau\rangle N_{\text{beams}})$ (once again the same procedure also applies to rotating arrays) (28) can be rewritten as

$$t_B^u = \frac{\kappa'}{N_{\text{elem}}^2 P_{\text{elem}} A_{\text{elem}}} \tag{34}$$

where $z \equiv N_{\text{elem}}^2 P_{\text{elem}} A_{\text{elem}}$ is the power-aperture product of an unweighted array and

$$\kappa' = 4\pi^2 R_{\max}^4 N_F kTDL \sin^2(\psi/2)/\sigma\eta^2. \tag{35}$$

Similarly we have for a weighted array

$$t_B^w = \frac{\kappa'}{z_w} \tag{36}$$

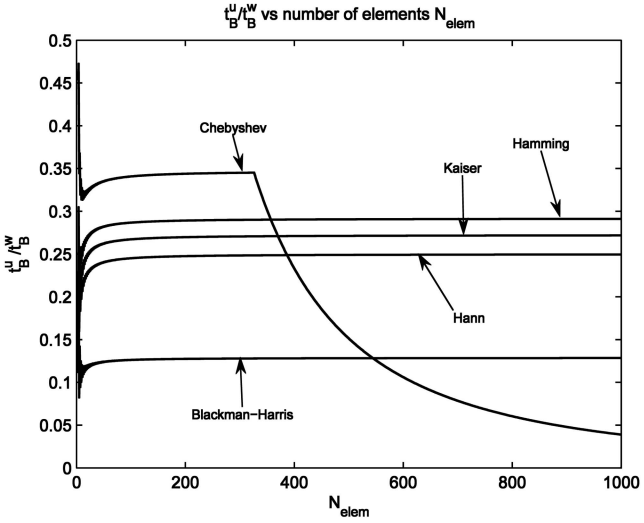

Fig. 4. Ratio of unweighted broadside dwell times t_B^u to weighted broadside side dwell times t_B^w using different windows is compared as function of number of elements. Chebyshev and Kaiser windows were calculated using sidelobe level (SLL) = −40 dB.

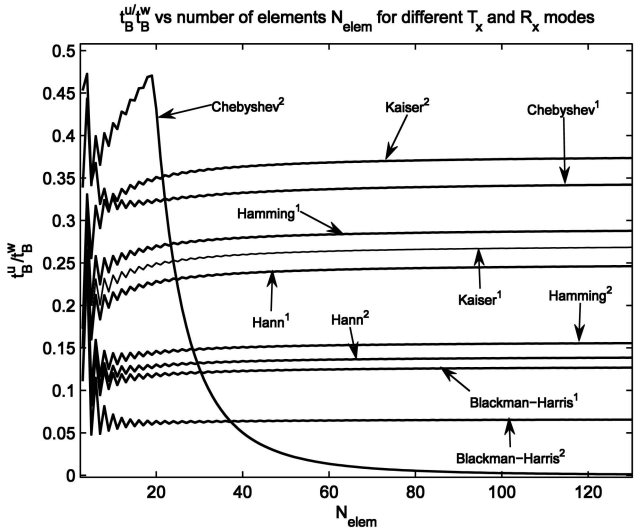

Fig. 5. Ratio of unweighted broadside dwell times t_B^u to weighted broadside side dwell times t_B^w versus number of elements for arrays with different weights for both transmit (T_X) and receive (R_X) modes. For windows with superscript (1) transmitted power is unweighted but reception is weighted. Sidelobe level (SLL) is chosen to be SLL = −40 dB for Chebyshev and Kaiser windows. For windows with superscript (2) both transmit and receive modes are weighted and here SLL = −20 dB for Chebyshev and Kaiser windows.

where z_w is the weighted power-aperture product. Dividing (34) by (36) gives the ratio

$$\frac{t_B^u}{t_B^w} = \frac{z_w}{N_{\text{elem}}^2 P_{\text{elem}} A_{\text{elem}}}. \tag{37}$$

Let the power-aperture product of a weighted array be given as $z_w = P_{\text{array}} A_{\text{array}}$ where we define P_{array} to be the average power of the array and A_{array} to be the effective area of the array. Then we have

$$z_w = \left[\sum_{i=1}^{N_{\text{elem}}} a_t^{(i)} a_r^{(i)}\right]^2 P_{\text{elem}} A_{\text{elem}} \tag{38}$$

with P_{elem} as the average power of the unweighted element (assumed identical across the array), $a_t^{(i)}$ are the normalised amplitude weights applied on transmission to element i, $a_r^{(i)}$ are the normalised amplitude weights applied on reception to element i. Where the element normalisation is such that $\max(a_{t,r}^{(i)}) = 1$, it reflects the practical issue that the antenna weighting is normally achieved by attenuating an element. For an unweighted antenna $a_t^{(i)} = 1$ and $a_r^{(i)} = 1$, reducing the previous result to the well-known $z = N_{\text{elem}}^2 P_{\text{elem}} A_{\text{elem}}$ shown above. From (37) and (38) we have

$$\frac{t_B^u}{t_B^w} = \frac{1}{N_{\text{elem}}^2}\left[\sum_{i=1}^{N_{\text{elem}}} a_t^{(i)} a_r^{(i)}\right]^2. \tag{39}$$

We can define the relative efficiency ϵ of the weighted array to the unweighted array to be

$$\epsilon = \frac{1}{N_{\text{elem}}^2}\left[\sum_{i=1}^{N_{\text{elem}}} a_t^{(i)} a_r^{(i)}\right]^2 \frac{P_{\text{elem}} G_{\text{elem}}}{P_{\text{elem}} G_{\text{elem}}} \tag{40}$$

where G_{elem} is the gain of the unweighted element, (this is related to the window function loss [14]). Thus we finally have that the weighted broadside dwell time is related to the unweighted broadside dwell time by the inverse of the array efficiency,

$$t_B^w = \frac{t_B^u}{\epsilon}. \tag{41}$$

We find that for any given window the power-aperture product increases as the number of elements is increased except for the Chebyshev window which decreases beyond a critical point as the number of elements is increased. The reason for this is due to the fact that as the array size increases beyond a certain limit the Chebyshev weights must transfer power from the mainlobe to the sidelobes in order to maintain the required sidelobe ratio. Fig. 4 shows this in terms of the efficiency of the arrays for different windows. For all windows the efficiency "saturates" for large arrays except for the Chebyshev weights which drop significantly. Fig. 5 addresses the issue of whether for a given two-way sidelobe level it is more efficient to weight both transmission and reception or just the one, which is usually reception because of interference rejection considerations. Windows with superscript 1 represent an unweighted transmission and weighted reception of −40 dB (for Chebyshev and Kaiser). On the other hand windows with superscript 2 represent the case of both transmit and receive modes being weighted and with −20 dB sidelobes for the Chebyshev and Kaiser windows.

Broadly speaking, the efficiency is greatest for all cases when the transmit mode is unweighted and the receive mode is weighted except for the Chebyshev window applied to small arrays where both T_x and R_x are the most efficient. From these results we can determine the behaviour of the unweighted broadside dwell times for the different subregions (see Table V for example), to the case where they are weighted by different window functions. Equation (41) and Figs. 4 and 5 show in particular that rotating arrays have better system performance charactersitics than static phased arrays but this is only true if the same window functions are used in order to carry out the comparison. If the wrong window function is chosen it is evident that this could lead to the reverse scenario where a static array outperforms a rotating array. Thus the choice of windows is critical in discerning the differences between the two systems.

VI. CONCLUSION

We have developed a method for determining the search functions for static and rotating phased array radars that in turn has allowed us to investigate the surveillance occupancy of different subregions. Rotating phased arrays give greater flexibility in the selection of the broadside dwell time needed to scan different subregions under varying constraints compared with the static array case. Rotating arrays also require less R_x and T_x elements to perform surveillance although this difference is decreased as N_F increases. Finally, we examine what effect the weighting of arrays has on the broadside dwell times and therefore how the performance differences can be reversed if different window functions are used.

A. ALEXOPOULOS
A. SHAW
Defence Science and Technology Organisation
Electronic Warfare and Radar Division
PO Box 1500, 180L
Edinburgh 5111
Australia
E-mail: (Aris.Alexopoulos@dsto.defence.gov.au)

REFERENCES

[1] Van Trees, H. L.
Optimum Array Processing.
New York: Wiley-Interscience, 2002.

[2] Corey, L. E.
A graphical technique for determining optimal antenna geometry.
IEEE Transactions on Antennas and Propagation, **AP-33** (1985), 719–726.

[3] Best, J. A.
Phased array coordinate transformations.
The Microwave Journal, (1962).

[4] Butler, J. M.
Tracking and control in multi-function radar.
Ph.D. dissertation, University College London, UK, 1998.

[5] Von Aulock, W. H.
Properties of phased arrays.
Proceedings of the IRE, **48** (1960), 1715–1727.

[6] Pearson, F.
Map Projections: Theory and Applications.
Boca Raton, FL: CRC Press, 1990, 195.

[7] Moon, P., and Spencer, D. E.
Field Theory Handbook: Including Coordinate Systems, Differential Equations and Their Solution (2nd ed.).
New York: Springer-Verlag, 1988.

[8] Alexopoulos, A.
Closed-form solutions for number of beams in static and rotating phased array radars.
Electronics Letters, **42** (2006), 822–824.

[9] Hannan, P. W.
The element-gain paradox for a phased array antenna.
IEEE Transactions on Antennas and Propagation, (1963), 423–433.

[10] Barton, D. K.
Modern Radar System Analysis.
Norwood, MA: Artech House, 1998.

[11] Kaiser, J. F.
Nonrecursive digital filter design using the I_0-sinh window function.
In *Proceedings of the IEEE Symposium on Circuits and Systems*, 1974, 20–23.

[12] Harris, F. J.
On the use of windows for harmonic analysis with discrete Fourier transform.
Proceedings of the IEEE, **66** (1978), 51–84.

[13] Oppenheim, A. V., and Schafer, R. W.
Discrete-Time Signal Processing.
Upper Saddle River, NJ: Prentice-Hall, 1989, 447–448.

[14] Nathanson, F. E.
Radar Design Principles (2nd ed.).
New York: McGraw-Hill, 1991. Reprinted by SciTech Publishing, 1999.